TISSUE ENGINEERING: Part A
Volume 20, Numbers 3 and 4, 2014

DOI: 10.1089/ten.tea.2013.0383

# Distraction-Induced Intestinal Growth: The Role of Mechanotransduction Mechanisms in a Mouse Model of Short Bowel Syndrome

Ryo Sueyoshi, MD, Kathleen M. Woods Ignatoski, PhD, Manabu Okawada, MD, and Daniel H. Teitelbaum, MD

Novel strategies are needed to address the problem of patients with short bowel syndrome. We previously demonstrated a three-fold lengthening of pig bowel after 2 weeks of applied distractive forces, but we have not elucidated the mechanisms facilitating this growth. We used a mouse model of distraction-induced enterogenesis. High molecular weight polyethylene glycol (PEG) osmotically stretched an isolated small bowel segment (PEG-stretch). Significant increases in villus height and crypt depth and in intestinal epithelial cell length and numbers suggested epithelial remodeling in addition to proliferation during enterogenesis. LC-MS/MS analysis showed a two-fold upregulation of α-actinin-1 and -4. We also demonstrated that p-focal adhesion kinase (FAK), FAK, α-actinin, and Rac1 were significantly upregulated and that F-actin was relocalized in PEG-stretch versus controls. Blockade of the phosphotidyl inositol 3′ kinase pathway failed to influence the increase in proliferation or decline in apoptosis after stretch, suggesting alternative signaling pathways are used, including MEK and P38MAPK, which were both upregulated during enterogenesis. Our data suggests that several known mechanotransduction pathways drive distraction-induced enterogenesis.

## Introduction

Short bowel syndrome (SBS) is the loss of significant small intestine length resulting in an inability to enterally absorb sufficient nutrients and electrolytes essential for survival. SBS has an incidence of 3–5 per 100,000 births per year[1] and is associated with significant complications and a reduced quality of life.[2] Patient outcomes have been linked to the length of remaining small intestine[3]; therefore, surgical procedures have been developed to increase bowel length.[4–6] However, the success of these procedures has been limited by surgical complications and reliance on dilated, dysfunctional bowel.[7] Small bowel transplantation, while a potential option, has limited success as well, with graft failure and rejection approaching 55% at 5 years.[8] To date, many patients with SBS rely on supplemental or total parenteral nutrition (TPN). However, TPN, or complete reliance on parenteral nutrition without feeding, has several complications, such as metabolic derangements, catheter-related morbidity, and sepsis.[2,3] Thus, new treatments for SBS are needed.

Successful small intestine elongation has been described using linearly-directed distractive mechanical forces, termed distraction-induced enterogenesis.[9–11] Previously, we demonstrated a 2.7-fold increase in bowel length over 10 days using an implanted hydraulic piston device in a pig model.[12] Physiologic function was retained in the lengthened gut after reimplantation, including motility, epithelial barrier function, mucosal disaccharidase levels, and electrophysiologic measures.[13] Further, reimplantation of the bowel into normal intestinal continuity demonstrated preservation of lengthening.[13,14] As this technique continues to be developed for clinical application in treating SBS, the mechanisms by which distraction-induced enterogenesis occur are unknown. Potentially understanding these mechanisms may lead to modalities to optimize this potential approach to SBS.

To best determine the mechanisms of action, we have developed a mouse model of distraction-induced enterogenesis. Previously we determined that the use of high molecular weight polyethylene glycol (PEG) instilled into the isolated small bowel led to osmotic movement of water into the lumen, accomplishing enterogenesis associated with an increase in cell proliferation compared to controls.[15] We used this mouse model to perform biased and unbiased investigative approaches to identify mechanistic pathways involved in distraction-induced enterogenesis. Our study demonstrates novel insights into the mechanisms and signaling pathways that are utilized during enterogenesis.

Section of Pediatric Surgery, Department of Surgery, University of Michigan Health System, Ann Arbor, Michigan.

## Materials and Methods

All animal experiments were conducted with approval from the University of Michigan Committee on the Use and Care of Animals (protocol number 07703/03986).

### *Animals*

Specific pathogen-free, male, 10–12-week old C57BL/6J (Jackson Laboratory) mice were used with body weight being >22.0 g. We also used a unique phosphotidyl inositol 3′ kinase (PI3K) knockout mouse which lacked the p85 subunit within the intestinal epithelium, using a Cre/Villin transgenic strain (kindly provided by V. Cohran).[16] A minimum of nine wildtype mice and/or three p85 Villin-knock-out (KO) mice were studied per group. Mice were maintained in a 12 h day/night rhythm at 23°C and a relative humidity of 40%–60%. Animals were fed standard rodent chow (LabDiet 5001 Rodent Diet; PMI Nutrition International, LLC) *ad libitum*. Forty eight hours before surgery chow was changed to microstabilized rodent liquid diet (TestDiet) to avoid postoperative obstruction from solid chow, while providing matched nutritional delivery.

### *Surgical method*

Anesthesia was induced by inhalational administration of 5% isoflurane and maintained by inhalational administration of 2% isoflurane. The abdomen was shaved and prepared with alcohol. A 2 cm midline incision (as small as possible) was made, and the ligament of Treitz was identified. For the PEG-stretch group, a well-vascularized segment (including at least two mesenteric arteries), 5 cm distal to the ligament of Treitz, was isolated on its mesenteric pedicle. The mean length was ~3.0 cm. PEG (Merck, PEG: 3350kDa; 350 μL) was gently injected into the isolated segment of small intestine, using silastic laboratory tubing (ID: 0.64 mm, OD: 1.19 mm; Instech Laboratories, Inc.) that was inserted inside the lumen of the isolated segment. After PEG injection, the catheter was gradually removed and the distal side was closed using a 6-0 silk sutures. The isolated segment was returned to the abdomen. Intestinal continuity was then reestablished by anastomosing proximal and distal jejunum in an end-to-end fashion with interrupted sutures (9-0 nylon). A similar approach was used for the control group; however, no injection was performed. In our previous work,[15] we found that injected saline was rapidly absorbed into the control segment, with no distension observed within postoperative days 3 and 5. Based on these earlier findings, we felt that any control injection would not influence the control group, and therefore, saline was not used in the control group for this study. 1.5 mL of 0.9% saline solution was injected to the peritoneal cavity before closing. Peritoneum and skin were closed using 4-0 polyglactin sutures (Fig. 1).

Mice were given microstabilized rodent liquid diet and 5% dextrose water postoperatively ad libitum. Mice were euthanized on postoperative day 5. Morphological changes (length and diameter) were recorded from the distended intestinal segments and a segment of normal intestine at the time of harvest.

Two 0.5 cm segments from the distended intestine were excised and placed into 10% formaldehyde. These segments were processed in paraffin, sectioned transversely, (5 μm) and stained with hematoxylin and eosin or immunofluorescence staining (IF). The remaining segment was immediately processed for real-time (RT)-PCR and protein analysis.[17]

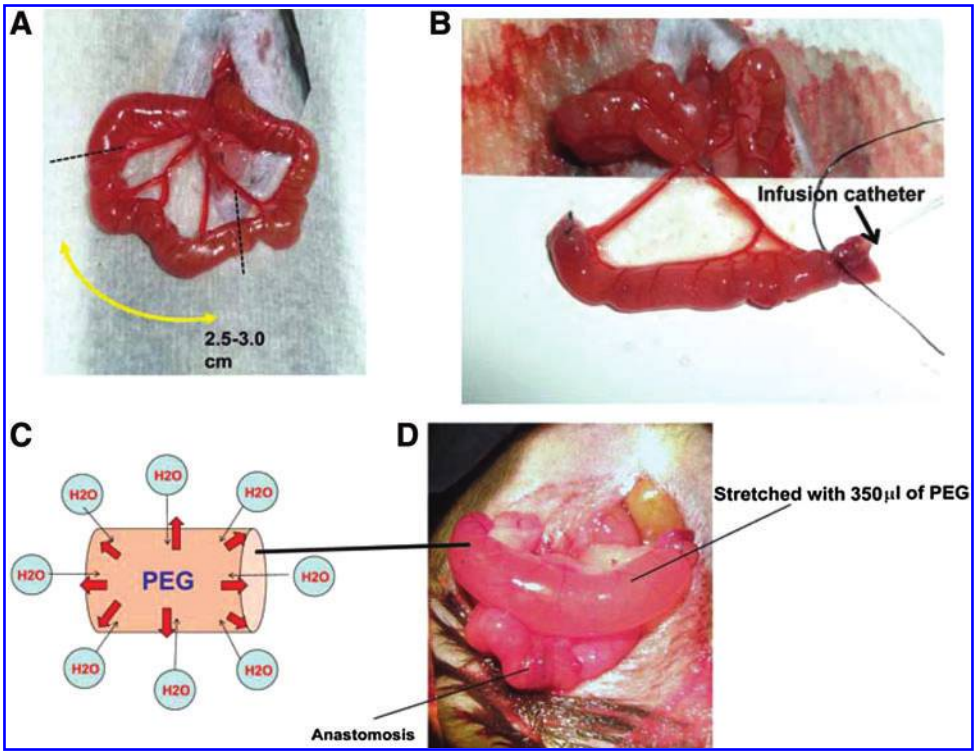


**FIG. 1.** Mouse model of distraction-induced enterogenesis. **(A)** After the small intestine was brought out of the peritoneum, a 2.5–3.0 cm segment of small bowel was isolated. **(B)** The catheter was then inserted into the isolated segment and 350 μL of polyethylene glycol (PEG) was injected thorough the catheter. Then the catheter was removed and the end sutured closed. **(C)** Based on osmotic forces, the PEG pulled abdominal fluid into the intestinal lumen (Black arrows). The red arrows indicate the distractive force forward to intestinal wall. **(D)** Final image of the stretched segment after the PEG injection at the time of surgery. Color images available online at www.liebertpub.com/tea

### Real-time PCR

Scraped intestinal mucosal tissue was placed into TRIzol (Invitrogen) and homogenized. cDNA was purified and processed as previously described.[17] All primers were designed on primer-BLAST website. Focal adhesion kinase (FAK), Talin1, Paxillin, Rac1, RhoA, and Vinculin, were examined. RT-PCR was performed using a Rotor-Gene 6000 (Corbett Life Science), and 18S RNA was used as an internal control for normalization. Fold changes of target genes were calculated using comparative quantification to 18S RNA. Primer sequences are

FAK: forward, 5-CTATCAACAGGTGAAGAGTGAC-3, and reverse, 3-CTTGACAGAATCCAGTAAACTC-5.

Rho A: forward, 5-AGCGTCTAGCTCTCAGGGCGT-3, and reverse, 3-ACGCGCGCACACTCTCAGT-5.

Paxillin: forward, 5-TCCGCAGCGAGTCACCTCCA-3, and reverse, 3-TCCCTGGGCCATGAACTTGAA-5.

Talin1: forward, 5-ATCCTTGTCCGCCTTCGCCTC-3, and reverse, 3-AGCTCTGGAGAGAACGCCCGA-5.

Rac1: forward, 5-TTTGGGTGGTGGCTGCTGCTG-3, and reverse, 3-CCCACCACCACACACTTGATGGC-5.

Vinculin: forward, 5-CAGAGTCACTGGGGTGTTAT-3, and reverse, 3-ATGCAGCACTTCAGCTCAGA-5.

### Two-dimensional gel electrophoresis

Mucosal protein was collected from isolated segments by mucosal scraping ($n=3$/group) and analyzed by 2D gel electrophoresis.[18] The 2D electrophoresis was performed by Kendrick Lab, Inc. Mucosal protein samples were lysed in 250 μL each of the osmotic lysis buffer (10 mM Tris, pH 7.4, and 0.3% sodium dodecyl sulfate [SDS]. Proteins in solution at a final concentration of 2.0 mg/mL) containing nuclease, phosphatase inhibitors, and protease inhibitors. 150 μL of SDS boiling buffer (5% SDS, 5% β-mercaptoethanol [BME], 10% glycerol, and 60 mM Tris, pH 6.8. Protein in solution at a final concentration of 35 mg/mL) without BME was added, and the samples were pulled repeatedly through 16 gauge needle and treated with Omnicleave. The samples were then heated in a boiling water bath for 5 min before protein determinations were performed using the bicinchoninic acid assay.[19] Samples were then diluted to 1.0 mg/mL in 1:1 diluted SDS boiling buffer: Urea sample buffer before loading.

Samples were then applied to the top of a thin tube gel containing 2% ampholines, and isoelectric focusing was carried out overnight, as previously described.[20] After a brief equilibration in SDS buffer, the tube gel was sealed to the top with a stacking gel overlaying a slab gel, and SDS slab gel electrophoresis was carried out for 4–5 h, followed by Coomasie Blue staining and drying. A total of 735 polypeptide spots from 2D gels were analyzed in this procedure. The differences between spots were measured from the spot density. Parametric analysis was used to calculate $p$-values, and each sample underwent a duplicate gel electrophoresis to insure accuracy.

### Mass spectrometry

We selected 15 spots, 5 upregulated and 10 downregulated, from 2D gels that were significantly (differentially expressed) different between the PEG-stretch and control groups, and these subsequently underwent analysis using mass spectrometry (LC-MS/MS) protein identification. Excised 2D spots were destained with 30% methanol and in-gel digestion was carried out as previously described.[21] Resulting peptides were resolved on a reverse phase C18 nano-LC column at a flow rate of 300 nl/min using 1% acetic acid/95% acetonitrile gradient system. Eluent was directly sprayed onto an Orbitrap XL (ThermoFisher) mass spectrometer using a nanospray source. Orbitrap was operated in a double play mode to collect a high resolution MS spectra (FWHM 30,000@400 m/z) followed by nine MS/MS spectra. Raw files were converted to mxXML format and searched against Uniprot mouse protein database appended with reverse sequences (decoy) and common contaminant proteins, using x!Tandem/TPP software suite. All proteins with a *ProteinProphet* probability of $<0.9$ (False discovery rate $>1\%$) and at least two corresponding peptides in the assay were considered positive identifications.

### Staining for mechanotransduction factors, proliferation, and apoptosis

Paraffin sections were stained as described previously.[22] Primary antibodies used for IF were α-actinin (1/100; Sigma) and p-FAK (1/200; Santa Cruz Biotechnology). Secondary antibodies were goat anti-mouse 488 IgG1 (1/500; Invitrogen) and goat anti-rabbit Texas red (1/500; Promega). A 4′,6-diamidino-2-phenylindole counterstain was used for nuclei detection.

For F-actin staining, sections were unmasked by citrate at 95°C. After two PBS washes, the sections were fixed in 4% formalin for 20 min, then washed and incubated in 0.1% Triton X-100 with PBS for 3 min to permeabilize cell membranes. The sections were then incubated in Texas Red® Phalloidin (1/40; Invitrogen) for 20 min to stain for actin. Paraffin sections were also stained with proliferating cell nuclear antigen antibody (1/1000; Cell Signaling Technology) for the assessment of cell proliferation. Secondary antibody was goat anti-mouse IgG 2a (1/1000; Invitrogen). For the assessment of cell apoptosis, TUNEL staining was performed using Apoptag®Plus Fluorescein In Situ Apoptosis Detection Kit (Millipore Corp.). The apoptosis index was determined the number of TUNEL positive cells in 100 crypts in each slide. If the detectable crypts did not fulfill 100 crypts, the ratio between positive cells and all crypts were used to produce an apoptosis index. All staining was visualized on a Nikon A1 confocal microscope (Nikon Instruments, Inc.) under 20× magnification.

### Protein (western) immunoblotting

Scraped tissues from intestinal mucosa were lysed in RIPA buffer (50 mM Tris, Ph 7.5; 150 mM NaCl, 1% Ipegal; 0.25% Na+ Deoxycholate; 10 μg/mL bovine serum albumin [BSA], 2 mM, ethylenediaminetetraacetic acid), containing 100 nM phenylmethanesulfonylfluoride, 0.2 μL/mL aprotinin, and 5 μL/mL leupeptin. After homogenization and centrifugation at 14000$g$ for 10 min at 4°C, the supernatant was stored in Læmmli loading dye. We used an immunoprecipitation procedure for FAK antibody as previously described.[23] Equal amounts of protein from whole cell lysates or equal amounts of immunoprecipitations were separated on 4%–20% SDS-polyacrylamide gels (Bio-Rad), and then transferred to a polyvinylidene difluoride membrane. Blots were blocked in 5% BSA and

Table 1. Histo-Morphologic Changes in Study Groups

| | *Stretch group* | *Control group* |
|---|---|---|
| Length | 139.2% ± 7.0%* | 110.7% ± 5.3% |
| Diameter | 166.4% ± 10.7%* | 126.1% ± 7.0% |
| Villus height | 350.1 ± 32.1 μm* | 279.1 ± 15.8 μm |
| Crypt depth | 105.6 ± 2.9 μm# | 85.3 ± 1.8 μm |

Results are the percent change from original length and expressed as mean ± SEM.

Length and diameter were compared between in operation and at the time of harvest.

*$p < 0.05$ for comparing with control group.

#$p < 0.01$ for comparing with control group.

$n = 6$ for all groups.

washed with Tris-buffered saline (TBS) containing 0.05% Tween (TBS-T) TBS-T. The membranes were incubated in each primary antibody (α-actinin [Sigma-Aldrich], phospho-FAK (Y397), FAK, Rac1, Phospho38 MAPK, AKT, phospho-AKT (Ser473), ERK,p p-ERK [Cell Signaling Technology], and GAPDH [Invitrogen]) overnight at 4°C. After three washes with TBS-T, the membranes were incubated for 1 h with secondary antibody. Then, after two washes with TBS- T, the membranes were developed for visualization of protein by the addition of enhanced chemiluminescence reagent according to the manufacturer's protocol (Supersignal®; ThermoScientific).

The α-actinin antibody was not specific for any one isoform (and thus detected both α-actinin 1 and 4); thus, we tested for all α-actinin on our blots and in our fluorescence (personal communication with the manufacturer).

### *Statistical analysis*

At least six animals were used per group per study, as determined by power analysis. Data are expressed as mean ± SD. Unpaired Two-tailed T Tests were used to compare the PEG-stretch results to the control group. A $p$-value < 0.05 was considered to be statistically significant.

## Results

Mechanical forces are crucial to the regulation of cell and tissue morphology and function.[24] Mechanotransduction is the process by which cells convert mechanical stress into chemical activity.[25] We used both biased and unbiased approaches to identify mechanotransduction signaling pathways which are activated in a PEG-stretched bowel.

### *Stretched bowel has increased length and diameter*

Isolated segments of mouse intestine were either PEG-stretch as induced osmotic forces from high molecular weight PEG, or noninjected as controls (Fig. 1). Length, diameter, villus height, and crypt depth were all measured in both study groups (Table 1). PEG-stretch segments were significantly longer (1.4-fold increase) and had significantly increased diameters (1.3-fold increase) compared to controls. Villus height was significantly increased in the PEG-stretch group (20.3%) compared to controls. Crypt depth was also significantly increased in the PEG-stretch group (19.2%) compared to controls.

### *Unbiased investigation of enterogenesis mechanisms*

A number of mechanotransduction pathways are known to activate cell proliferation and tissue growth. However, our initial direction to examine mechanisms driving this growth used a nonbiased approach to insure that other potential mechanisms were not missed. We analyzed a total of 735 protein spots in 2D gels to identify differential expression of proteins isolated from PEG-stretched and control mucosa. We selected 15 spots which were differentially expressed between the two groups as described in the Methods section. Five spots corresponded to upregulated proteins and 10 were downregulated proteins. The spots were excised from the gels, and mass spectrometry (LC-MS/MS) was performed to identify the proteins. Table 2 shows the identified proteins, as well as the functional attributions of these. Interestingly, virtually all of these proteins identified, regardless of the direction of expression (up or down) related to either integrin signaling (Up: Integrin beta-4) and protein

Table 2. Mass Spectrometry Analysis of Isolated Proteins from 2D Gel Electrophoresis

| | *Protein name* | *Regulation (Difference)* | *Function* |
|---|---|---|---|
| 1 | Alpha-actinin-1 | Upregulated (2.6) | Binds actin to integrin receptor |
| 2 | Alpha-actinin-4 | Upregulated (2.6) | Binds actin to integrin receptor |
| 3 | Heat shock protein 90 β1 | Upregulated (1.9) | Assists in protein folding |
| 4 | Gelsolin | Upregulated (2.0) | Promotes actin polymerization |
| 5 | Integrin beta-4 | Upregulated (1.8) | Assembly hemidesmosome |
| 1 | Cytoskeleton-associated protein 4 | Downregulated (−3.0) | Interact directly with α-actinin |
| 2 | Beta-actin | Downregulated (−2.7) | Nonmuscle cytoskeletal actin |
| 3 | Actin, gamma, cytoplasmic 1 | Downregulated (−1.9) | Nonmuscle cytoskeletal actin |
| 4 | Tropomyosin 2 protein | Downregulated (−2.6) | Regulate the interaction of actin and myosin |
| 5 | Actin cytoplasmic2 | Downregulated (−2.3) | Maintain the cytoskeleton |
| 6 | Actin, cytoplasmic 1, N-terminally | Downregulated (−2.0) | Maintain the cytoskeleton |
| 7 | Replication factor C | Downregulated (−2.1) | Protein complex that is required for DNA purification |
| 8 | Methylmalonyl-Coenzyme A mutase | Downregulated (−2.2) | Catalyze enzyme from methylmalonyl-CoA to succinyl CoA |
| 9 | Alpha-actin | Downregulated (−1.8) | Skeletal actin |
| 10 | Ornithine aminotransferase | Downregulated (−1.9) | Enzyme involved in the ultimate formation of proline from orthinine |

Table 3. mRNA Expression

| | *PEG-stretch group* | *Control group* |
|---|---|---|
| FAK | 19.9 ± 3.1 | 13.4 ± 2.2 |
| Rho A | 4.9 ± 0.8 | 12.8 ± 0.8 |
| Rac1 | 11.1 ± 1.5* | 5.3 ± 0.6 |
| Paxillin | 23.9 ± 4.3 | 18.7 ± 3.8 |
| Talin1 | 6.2 ± 0.6 | 6.8 ± 0.3 |
| Vinculin | 153.6 ± 48.5 | 96.5 ± 9.8 |

Results are expressed as mean ± SEM.
Fold changes of target genes were calculated using comparative quantification to 18S RNA.
*$p < 0.05$ compared to control group.
PEG, polyethylene glycol.

formation or folding (Up: Heat shock protein 90 β1 and Down: Ornithine aminotransferase); but a predominant number of proteins related to cellular actin cytoskeletal structure (Up: Alpha-actinin-1, Alpha-actinin-4; Down: Cytoskeleton-associated protein 4, Beta-actin, Actin gamma cytoplasmic 1, Gelsolin, Tropomyosin 2 protein, Actin cytoplasmic 2 and Actin cytoplasmic 1 N-terminally Alpha-actin).

Because we were primarily focused on studying force-induced enterogenesis, we deliberately selected for further investigation the family of proteins showing the greatest degree of upregulation, α-actinin-1, and α-actinin-4, which were both increased 2.6-fold in the PEG-stretch group compared to controls. Both proteins have been previously demonstrated to be involved in mechanotransduction regulation.[26] We then focused our directed investigation on proteins centered on remodeling of the actin cytoskeleton.

### *Directed investigation of enterogenesis mechanisms*

Given that a number of proteins related to mechanotransduction were found to be differentially expressed during distraction-induced enterogenesis, we next determined the mRNA expression level (Table 3) of several factors associated with known mechanotransduction pathways, including FAK, Rho A, Rac1, Paxillin, Talin1, and Vinculin. FAK, Paxillin, and Vinculin mRNA were slightly increased in the PEG-stretch group, and Rac1 expression was significantly increased in the PEG-stretch group compared to controls ($p < 0.05$).

The increase in protein expression of α–actinin (from MS/MS analysis), as well as the mRNA expression for Rac1 and FAK (including the active form, phospho-FAK), were next confirmed by western immunoblotting (Fig. 2A). Rac1, α–actinin, and phospho-FAK were all significantly upregulated in the PEG-stretch group compared to controls. It is noted that FAK was below the detectable limit in the control group. Thus, we analyzed total FAK expression from naïve mouse tissue, which did not undergo any surgical manipulation, and identified a baseline expression of total FAK, which was lost in nondistended control segments. The increased phospho-FAK expression found in the PEG-stretch group was comparable to the level of phospho-FAK found in normal functioning bowel in the naïve group. This suggests that the isolation of an intestinal segment, without mechanical stimulation results in a profound loss of critical mechanotransduction proteins; whereas the stimulation with mechanical PEG-stretching resulted in a preservation of total FAK, as well as an upregulation of phospho-FAK. This is consistent with our previous observation that there is morphological atrophy of the crypt/villus complex in the isolated control segment compared to the PEG-stretched segment.[15]

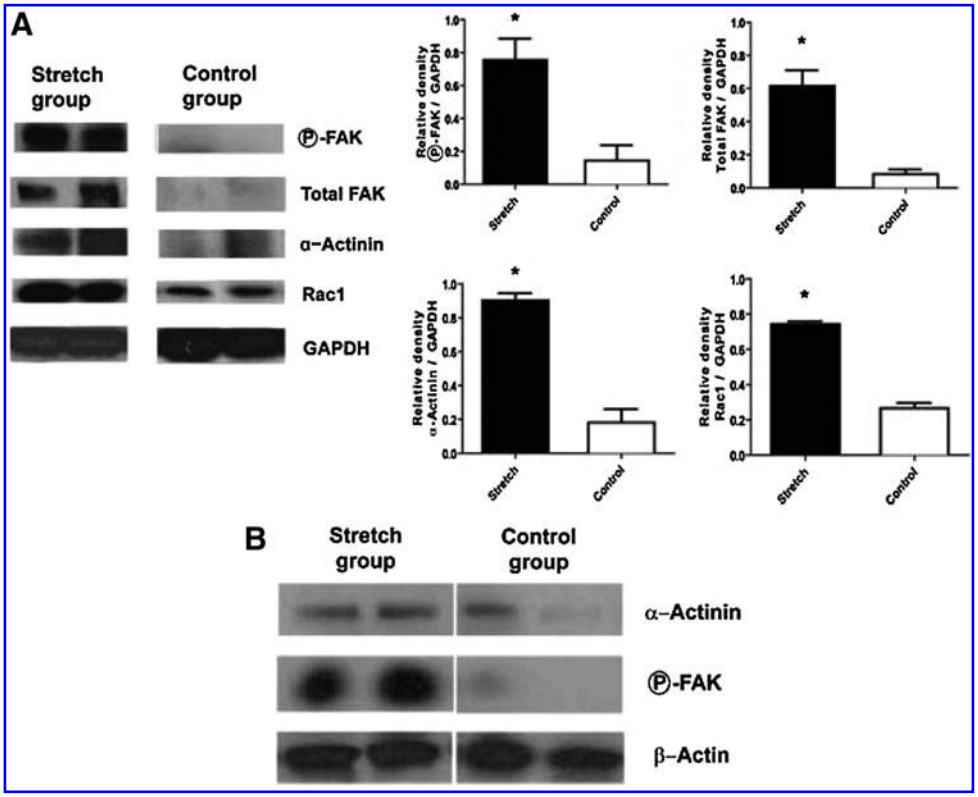


**FIG. 2.** Rac1, focal adhesion kinase (FAK), and α-actinin protein levels were increased and relocalized in PEG-stretched compared to control intestine. **(A)** Whole cell lysates were prepared for both PEG-stretched and control intestinal segments and probed using western blot technology. GAPDH was used as a loading control. Rac1, phospho-FAK, and α-actinin were significantly increased. **(B)** By FAK immunoprecipitation and western blotting, we determined that α-actinin was in a complex with FAK in the PEG-stretched intestines as opposed to in the control segments. *$p < 0.05$; $n =$ a minimum of six per group.

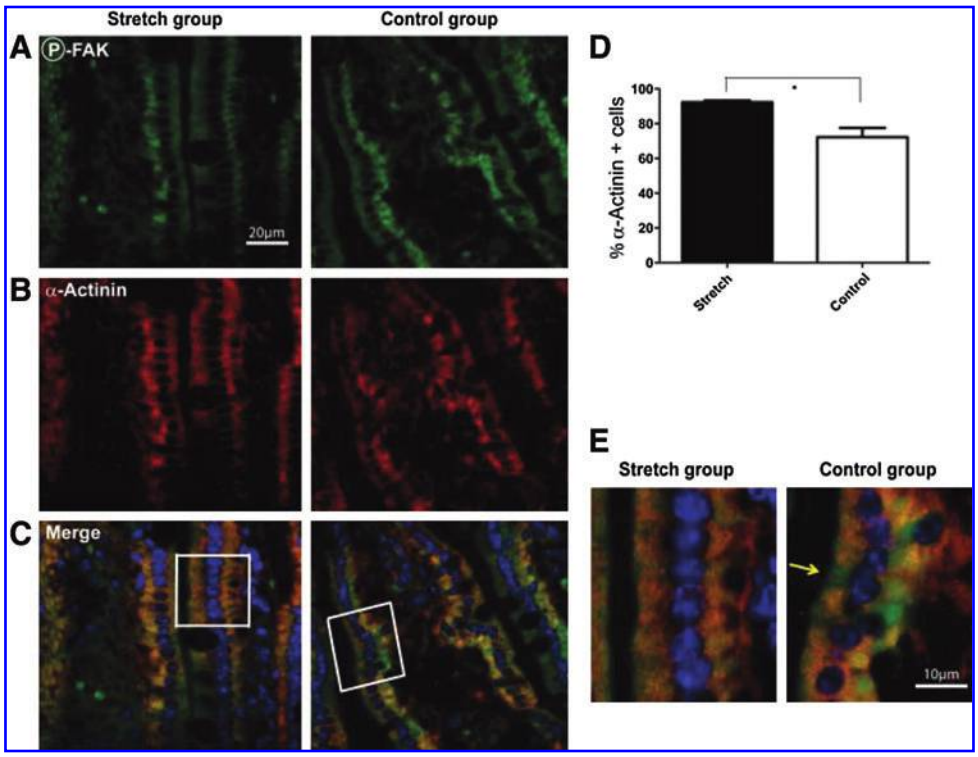


**FIG. 3.** α-actinin relocalized in PEG-stretched intestine compared to control intestine. Phospho-FAK and α-actinin were visualized by immunonofluorescence staining (representative sections are shown in **A** and **B**, respectively); combined images are in **C**. White boxes in **C** indicate areas shown in **E** Almost all of EC cells stained for α–actinin in the PEG-stretched group **(D)**; on the other hand, some of the control EC cells did not stain **(D, E**, yellow arrow**)** (PEG stretch: 92.3%±2.2%, Control: 72.2%±13.9%). *$p<0.05$; $n=$a minimum of six per group. Color images available online at www.liebertpub.com/tea

### *FAK complexes with α-actinin with distraction-induced growth*

Since it is known that FAK works in a complex with α-actinin and Rac to promote cell motility and growth,[27,28] we determined if FAK was in such an associated complex when the intestine were stretched. Using FAK immunoprecipitation assays and western blotting, we identified α-actinin is in a complex with FAK in the PEG-stretch group as opposed to controls (Fig. 2B). Our results suggest that the FAK/α-actinin complex is used to promote enterogenesis. Because this complex has been shown to rearrange the actin cytoskeleton,[29,30] we also determined if actin was present in the complex. As seen in Figure 2B, actin is also found to be present in this complex.

Since we identified an increase in the expression of the α-actinins in our PEG stretch model (Table 2), we further examined what other proteins might interact with α-actinin. α-actinin cross-links F-actin fibers forming a complex attached to focal adhesions (FAs) that can guide the cell during attachment and detachment associated with movement and proliferation.[26,31] Thus, both α-actinin and F-actin can be relocalized during such cellular processes.[27] Since the bowel is increased in diameter and length, and both the villus height and crypt depth were also increased (Table 1), indicating an increase in cell movement and proliferation, we hypothesized that α-actinin would be relocalized in the PEG-stretch model compared to controls. Therefore, we examined the localization of α-actinin in PEG-stretch versus control segments. α-actinin was uniformly found in the cytoplasm of almost all intestinal epithelial cell (IEC) in the PEG-stretch group colocalizing with p-FAK, but was identified in a reduced number of IEC in the control group, and had decreased intensity of staining in controls (Fig. 3). Quantification showed that 92.3%±2.2% of the IEC cells in the PEG-stretch group contained α–actinin; whereas, only 72.2%±13.9% ($p<0.05$) contained α–actinin in the controls.

### *Stretching induced cell polarization changes*

Cell growth was accompanied by changes in the actin cytoskeleton which could potentially result in changes in shape and polarization of the cells. Such mechanically-induced changes have been reported in other mechanotransduction models.[32–34] Thus, we next evaluated IEC length and numbers and the general physical appearance of the PEG-stretched intestines as compared to controls (Fig. 4A, B). The lengths of the IEC were statistically increased in the PEG-stretch group (21.2±3.1 μm) versus the control group (19.4±3.2 μm; $p<0.05$) (Fig. 4C). IEC were also flattened and elongated in the PEG-stretched segments compared to controls (Fig. 4A, B). In addition, the number of IEC per 100 μm of villus were significantly increased during enterogenesis (stretch group: 21.8±2.2, control group: 17.6±1.2; $p<0.05$) (Fig. 4D). These data suggest that enterogenesis resulting from distractive force facilitates an increase in cell proliferation, as well as cell movement and a restructuring of individual epithelial cells.

F-actin is the filamentous polymer of actin subunits that form α-actinin-linked stress fibers in the cell.[27] Epithelial cells have a basket-like network of stress fibers that breaks down into the actin subunits during various cellular processes.[35] Thus, as with α-actinin, F-actin could also be redistributed with changes in mechanical stretching; therefore, we next examined changes in F-actin localization. F-actin was localized to the cell membrane in both the PEG-stretch and control groups; however, F-actin formed a significantly thicker apical band in the PEG-stretch group than in the control group (PEG-stretch 1.88±0.21 μm, control 1.45±0.27 μm;

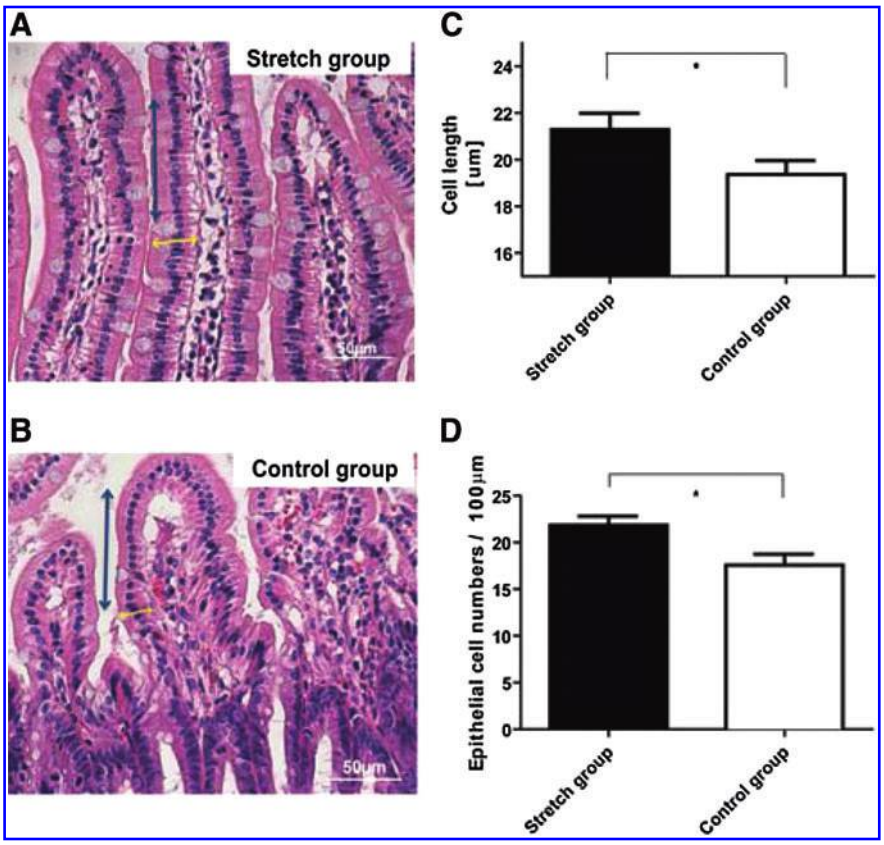


**FIG. 4.** Epithelial cells became elongated in the PEG-stretched group compared to controls. Representative hematoxylin and eosin staining of histological sections from both groups are shown **(A, B)**. Intestinal epithelial cell (IEC) length (yellow arrow) was significantly expanded in the PEG-stretch group versus controls. **(C)** Mean cell length, as determined by counting a minimum of 10 villus complexes in the PEG-stretched and control groups, is shown graphically ($p < 0.05$). **(D)** Total EC numbers were estimated by counting the number of cells in 100 μm of tissue (blue arrow) in a minimum of 10 villus complexes. *$p < 0.05$; $n$ = a minimum of six animals per group. Color images available online at www.liebertpub.com/tea

$p < 0.01$) (Fig. 5), indicating mechanical stretching resulted in a remodeling of the internal actin cytoskeleton.

### *Cell proliferation and apoptosis*

Intestinal atrophy in the control group along with the loss of PEG-stretch stimuli, and the loss of FAK may lead to anoikis. Therefore, we determined the status of the proliferative and apoptotic signaling pathways known to be downstream of FAK. It has been previously demonstrated that Rac1 signaling pathway activates AKT through p38MAPK.[36,37] Since we have shown that RAC changes in abundance and localization with stretch, we determined the expression of p38MAPK. Expression of p38MAPK increased in the PEG-stretch group compared to the Control group ($p = 0.08$) (Fig. 6); suggesting that this signaling pathway is activated in our model. Because the PI3K pathway and activation of AKT have been shown to play a role in apoptosis[38] and proliferation,[16] and are downstream of p38MAPK, we determined the expression and activation of AKT. The PEG-stretch group exhibited markedly increased phospho-AKT compared to the control group ($p < 0.05$) (Fig. 6). We also examined a known proliferation pathway that has been linked to FAK, the ERK pathway. Although the relative expression of phospho-ERK increased in the PEG-stretch group compared to the control group, it did not reach statistical significance ($p < 0.06$) (Fig. 6).

Based on the significant increase in phospho-AKT expression in the PEG-stretch group, we next explored the role of the PI3K pathway in distraction-induced enterogenesis. We used a p85 Villin-KO PI3K mouse which lacked the p85 subunit within IECs. The p85 Villin-KO mice subjected to PEG-stretch exhibited a significant increase of IEC proliferation (50.3% ± 5.0% PCNA positive crypt cells compared to all crypt cells) compared to p85 Villin-KO controls (39.7% ± 1.7%), $p < 0.05$; and this increase was not significantly different from PEG-stretch wildtype mice ($p = 0.23$) (Fig. 7A). Thus, an intact PI3K pathway is not needed to control proliferation during distraction-induced enterogenesis.

Given that AKT has been shown to play a role in protecting against apoptosis, we measured the rate of IEC apoptosis using TUNEL staining. The amount of apoptosis was increased in PEG-stretched p85 Villin-KO segments (44.9 ± 12.5) compared to the wildtype stretched segments (18.7 ± 5.6; $p = 0.06$). In addition, apoptosis was significantly increased in the control p85 Villin-KO segments (32.5 ± 2.5) compared to wildtype control segments (73.0 ± 18.4), $p < 0.05$ (Fig. 7B). These data were expected as AKT activation in the IEC from these intestines is greatly decreased (Feng, personal communication). However, there was still less apoptosis in the stretched p85 Villin-KO intestine than in the control ($p = 0.25$), indicating that the PI3K signaling pathway plays a role in controlling apoptosis during distraction-induced enterogenesis.

## Discussion

Cells in multicellular tissues are subjected to a myriad of forces, including compressive forces, tensile forces, fluid shear stress, and hydrostatic pressure, each of which plays an intricate part in the shaping, development, and maintenance of the tissue.[25] The process that brings about important cellular changes through such forces is termed

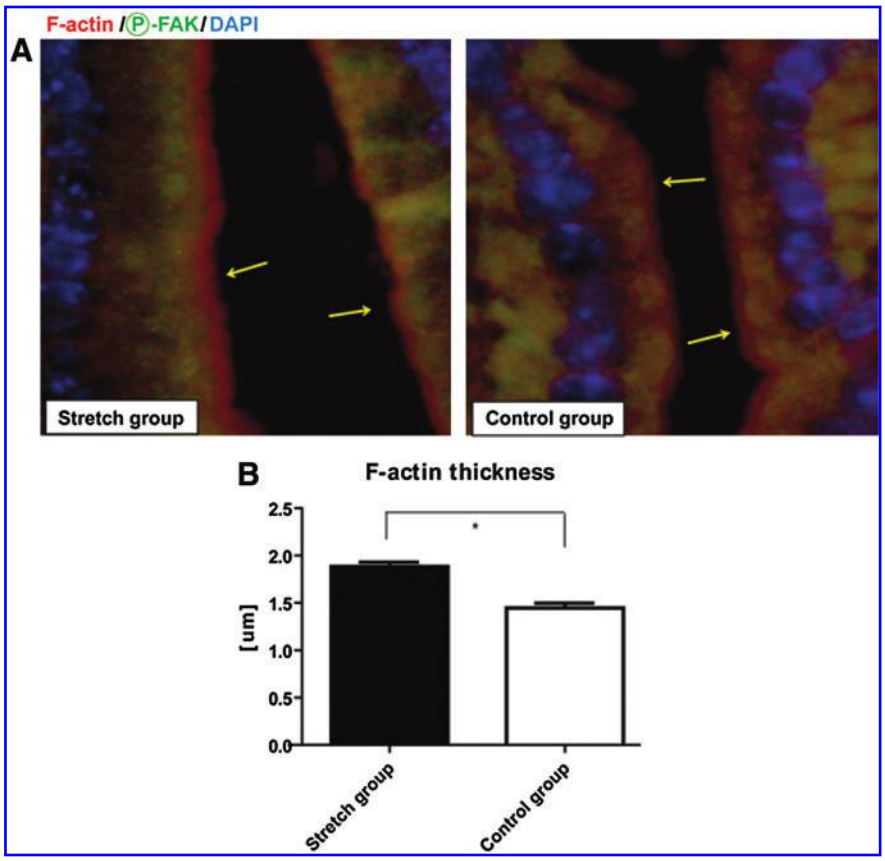


**FIG. 5.** F-actin relocalizes to the apical surface in stretched versus control intestinal segments. **(A)** F-actin and phospho-FAK were visualized by immunofluorescence; representative images are shown. Note the formation of a band of F-actin which was markedly thicker and longer in the PEG-stretch group compared to the control group (yellow arrows). **(B)** Graphical comparison of the measurement of the thickness of the F-actin band (mean ± SD; PEG-stretch 1.88 ± 0.21 μm, control 1.45 ± 0.27 μm). *$p < 0.01$; $n$ = a minimum of six animals per group. Color images available online at www.liebertpub.com/tea

mechanotransduction. Changes in cell shape, motility, cytoskeletal remodeling, and FA contacts have been the focus of several investigations.[39,40] It is known that cells can sense mechanical forces as a result of signals transmitted from extracellular matrix to intracellular biochemistry.[25] In particular, Hoffman, *et al.* described the mechanotransmision, mechanosensing, and mechanoresponse of intracellular signaling pathways for mechanotransduction.[39]

A critical consequence of SBS is loss of absorption area, so recent research has focused on increasing absorption area.[11,12,41,42] The use of growth factors may result in significant increase in bowel adaptation.[43] Using an implanted mechanical device in pigs, our laboratory demonstrated a far greater increase in adaptation than can be achieved with growth factors—nearly three-fold increase in small bowel length[12] In addition to lengthening of the bowel, epithelial cell

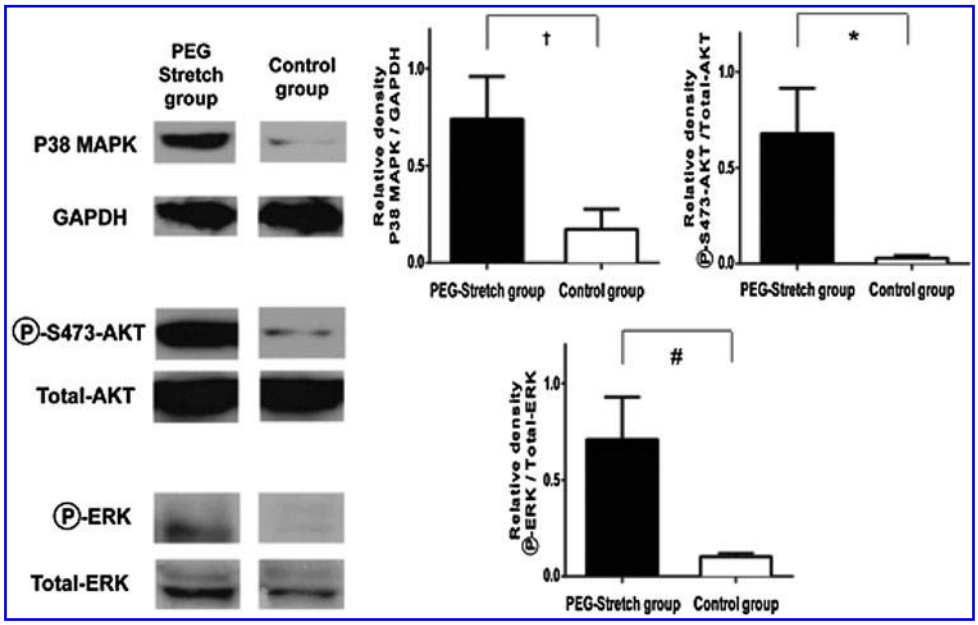


**FIG. 6.** FAK-associated cell proliferation signals are upregulated and apoptosis is decreased in the PEG-stretched segments. Proteins from whole cell lysates were probed for total p38MAPK, total and phospho-AKT (phosphorylated at Ser 473), and total and phospho-ERK. The PEG-stretch group exhibited markedly increased relative expression of p38MAPK (†$p = 0.08$) and significantly more phospho-AKT compared to the control group (*$p < 0.05$). Although the relative expression of phospho-ERK/total ERK increased in the PEG-stretch group compared to the control group, it did not reach statistical significance (#$p = 0.06$).

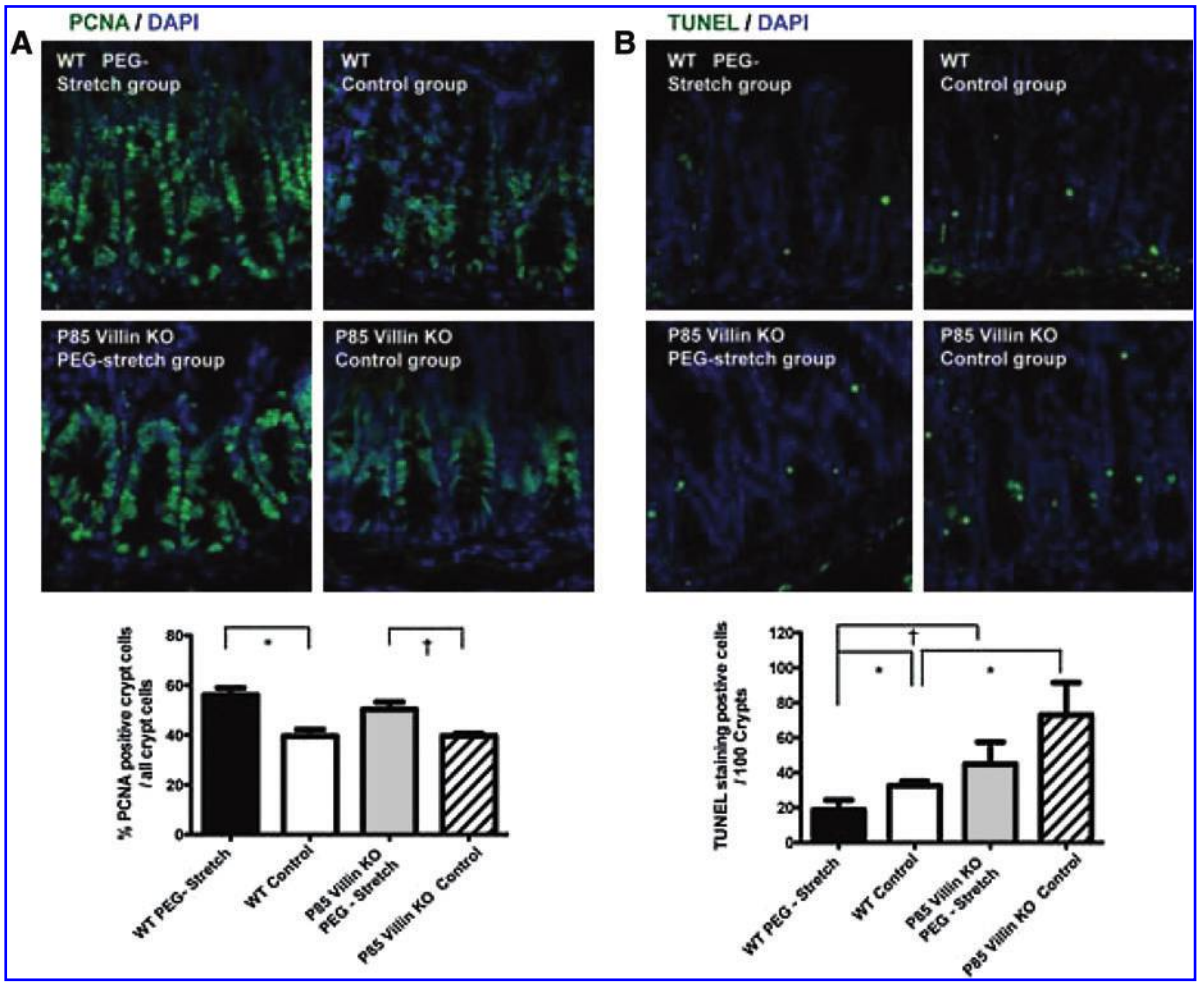


**FIG. 7.** Proliferation was increased and apoptosis was decreased in stretched segments compared to control. **(A)** PCNA staining of stretched and control segments in both wildtype and p85 Villin-Cre conditional IEC knock-out mice. Increased proliferation is seen in stretched segments but is not affected by deletion of phosphotidyl inositol 3′ kinase function. **(B)** Terminal deoxynucleotidyl transferase dUTP nick end labeling (TUNEL) staining of stretched and control segments in both wildtype and p85 Villen-Cre conditional IEC knock-out mice. Decreased apoptosis was seen in stretched segments compared to wildtype, but the ratio of apoptosis levels of stretched to control did not change. $^{*}p < 0.05$; $^{\dagger}p < 0.01$. Color images available online at www.liebertpub.com/tea

proliferation was stimulated in the lengthened segment. Concordant with the pig results, our laboratory also showed that cell proliferation was stimulated in the PEG-stretch mouse model of short SBS.[15] In this model, distractive forces were created outward by hydrostatic pressure to the intestinal wall of isolated segments. Despite demonstration of bowel lengthening in multiple models, the molecular mechanisms of enterogenesis by distractive force are still unknown.

The mechanism by which mechanotransduction occurs has been explored using *in vitro* models of various cell types, including osteocytes, chondrocytes, and cardiomyocytes.[32–34] In these models, activation of FAK drives the mechanotransduction pathways leading to increased bone growth and cardiac repair. The FA signaling cascade appears to be primarily mediated by the phosphorylation of FAK, which upon mechanical traction on extracellular integrins leads to one of the earliest markers to change activity with applied tension on the FA.[44]

Concordant with the results in cardiomyocytes and bone cells, Chaturvedi *et al.* have shown that FAK appears to be involved in healing of the gut mucosa.[45] Using human and rat intestinal cell lines and intestinal damage in the forms of ulcers and Roux-en-Y atrophy, they have demonstrated that strain causes the activation of Rac1 and or Src and FAK.[46] Activation of FAK then facilitates the activation of ERK, which in turn activates p38MAPK to produce motility and proliferation. Our results are consistent with these data in that we observe FAK and RAC 1 activation, which then turns on p38MAPK to promote proliferation and decrease apoptosis. However, our results were performed strictly *in vivo* with the intent of finding proteins that were activated during the stretch process. Thus, similar pathways are downregulated when atrophy is present that we are seeing upregulated when we are inducing growth. Interestingly, Kovalenko *et al.* also observed an upregulation of the same pathways in ulcer repair as we observed during stretching.[46] Concordant with this, Livant has shown that the same signals that occur in cells responding to a wound healing situation also are activated during cell growth and tumor metastasis.[47] Together, all these data indicate that similar mecahnotransduction pathways are activated in response to stimulation either by wound healing or by mechanical

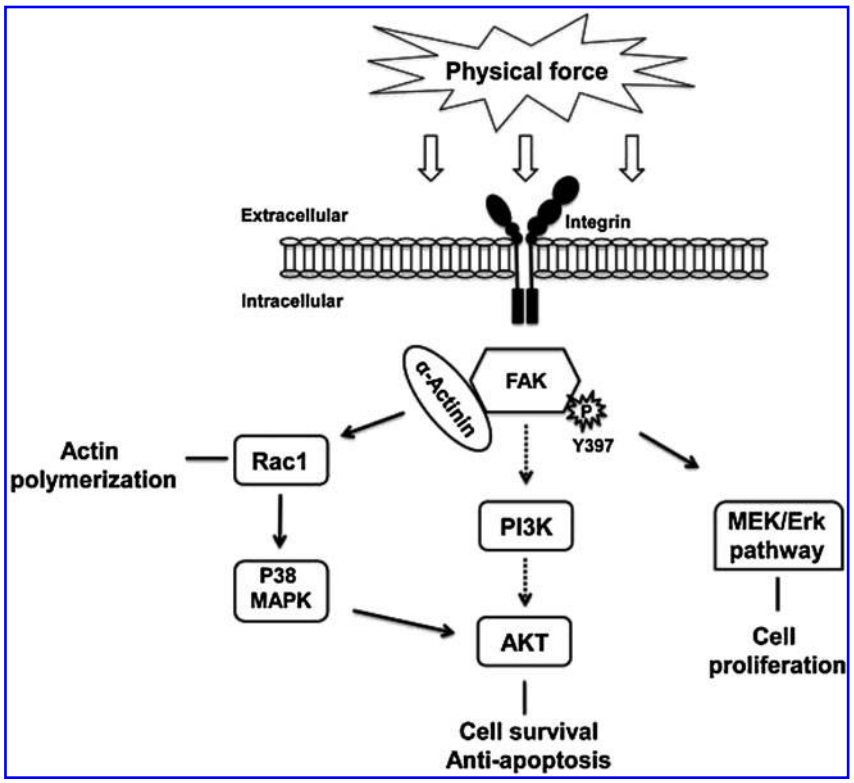


**FIG. 8.** Potential model of mechanotransduction forces driving enterogenesis. Based on the data presented here, physical force (potentially via cell membrane integrins) driving of the FAK pathway plays a central role in mechanotransduction during enterogenesis. FAK activation leads to a polymerization with α-actinin. This then leads to several downstream regulatory processes, including RAC-1 and cell shape changes. RAC has been shown to activate p38MAPK which can lead to AKT activation and decreased apoptosis. FAK activation also led to AKT and ERK activation facilitating proliferation and survival. Whether the cell shape change and the increase in cell proliferation and survival are directly linked remains to be addressed.

stretching, indicating that the wound healing pathways can be commandeered to further grow the intestine.

Our data suggest a role for FAK in mechanotransduction during distraction-induced enterogenesis and show an increase in several factors in the FAK signaling pathway used for cell motility and cell growth. FAK is an upstream mediator of Rac1-facilitated actin cytoskeleton rearrangement,[48] as well as a mediator of stress-induced mechanotransduction.[49] In fact, Rac1 was significantly upregulated in the PEG-stretch group compared to controls by RT-PCR and western blotting results. Moreover, our results showed F-actin was in a statistically thicker band on the leading edge in the PEG-stretch group than in the control group; demonstrating a remodeling of the intracellular actin structures during epithelial growth.

F-actin stress fibers are anchored in FAs[27] where the tyrosine kinase FAK resides. Activation of FAK signaling promotes cell shape changes through RAC1.[29] Detachment of FAs, rearrangement of the actin cytoskeleton, and cell shape changes are consistent with the involvement of FAK signaling in distraction-induced enterogenesis. We have shown the rearrangement of the actin cytoskeleton and activation of FAK, and concordant with other published data,[50] IECs of the PEG-stretched intestine were longer than the control group. In addition, IECs were not only lengthened but thinner in the PEG-stretched intestine, suggesting a change of shape and activation of proliferation during PEG-stretch, which were confirmed by PCNA staining.

Our results indicate that FAK is potentially using these two pathways to promote IEC growth and reduce apoptosis during enterogenesis. It has been demonstrated that FAK promotes both MEK/ERK and PI3K-AKT signaling pathways.[51,52] Our findings using the PI3K conditional intestinal KO mice demonstrated that AKT activation downstream of PI3K has a role in inhibiting apoptosis during enterogenesis. However, loss of PI3K did not significantly reduce the amount of apoptosis in the stretched segment compared to the controls, leading to the conclusion that another pathway may be involved in preventing apoptosis and promoting proliferation during stretch. Our data suggest, although do not verify, that the RAC/p38MAPK pathway may be involved. Future studies will determine the role of RAC/p38MAPK kinase in distraction-induced enterogenesis.

Interestingly, we failed to observe FAK expression in the control group in western blotting. The isolated segments of our control group did not have intestinal luminal contents, so those segments were not subjected to normal intestinal luminal pressure or the normal flow of enteric contents. Flanigan, *et al.* demonstrated that a defunctionalized intestine–Roux-en-Y distal segment had decreased cell proliferation and ERK activation due to less intestinal luminal pressure.[53] The intestinal luminal pressure may be critical for the intestinal cell growth and motility. Likewise, it is possible that such a loss of FAK may also exist in states where the gastrointestinal tract is in a condition of disuse, such as after major abdominal surgery. It is possible that manipulation of FAK in such states could lead to improved postoperative gastrointestinal function.

In this work, we have shown that similar mechanisms exist to repair the gut as are used in other systems where mechanotransduction is prevalent.[54] There are clearly several limitations to the current approach. While we took a broad, directed, as well as unbiased approach, other mechanotransduction pathways may well exist that might not be detected by these approaches. For instance, there were several areas of the 2D gel electrophoresis that may have been

beyond the point of detection of the authors. Further, it is also possible that protein amounts may be less relevant than their activation state (e.g., phorphorylated) or physical location within the cell, itself (e.g., submembrane vs. cytosolic). Thus, future work will need to consider an even broader examination of these mechanisms of action. A suggested model of the cellular pathways promoting enterogenesis from our current study is summarized in Figure 8. Mechanisms of mechanotransduction have been well studied in other systems and these mechanistic pathways appear to be similar in enterogenesis. We have previously shown using a pig model that we can use a mechanical device to induce distractive forces that then increase the absorptive area of the bowel. We have explored the use of distraction-induced growth for the clinical treatment of SBS, and have produced several potential approaches for a surgically implantable device, which might be used for such a purpose.[55] Alternative approaches, including magnetically-driven distraction, hydraulic devices, and the use of shape memory alloys may all have potential roles.[56] While the approach of using an osmotically-driven approach, as in the current article, has not been explored for clinical use, this is certainly a potentially viable approach. In the future, we would potentially like to enhance the mechanotransduction pathways during stretching induced by our device to enable the bowel to stretch further, achieving greater absorptive area in a shorter length of time and with less discomfort.

### Acknowledgments

We thank Pele Browner for the excellent technical assistance. This work was supported by NIH 2R01AI-44076-14; and The Hartwell Foundation via a Biomedical Research Grant.

### Author Disclosure Statement

No competing financial interests exist.

### References

1. DeLegge, M., Alsolaiman, M.M., Barbour, E., Bassas, S., Siddiqi, M.F., and Moore, N.M. Short bowel syndrome: parenteral nutrition versus intestinal transplantation. Where are we today? Dig Dis Sci **52,** 876, 2007.
2. Squires, R.H., Duggan, C., Teitelbaum, D.H., Wales, P.W., Balint, J., Venick, R., *et al.* Natural history of pediatric intestinal failure: initial report from the Pediatric Intestinal Failure Consortium. J Pediatr **161,** 723, 2012.
3. Spencer, A.U., Neaga, A., West, B., Safran, J., Brown, P., Btaiche, I., *et al.* Pediatric short bowel syndrome: redefining predictors of success. Ann Surg **242,** 403; discussion 9, 2005.
4. Bianchi, A. Intestinal loop lengthening—a technique for increasing small intestinal length. J Pediatr Surg **15,** 145, 1980.
5. Kimura, K., and Soper, R.T. Isolated bowel segment (model 1): creation by myoenteropexy. J Pediatr Surg **25,** 512, 1990.
6. Kim, H.B., Lee, P.W., Garza, J., Duggan, C., Fauza, D., and Jaksic, T. Serial transverse enteroplasty for short bowel syndrome: a case report. J Pediatr Surg **38,** 881, 2003.
7. Sudan, D., Thompson, J., Botha, J., Grant, W., Antonson, D., Raynor, S., *et al.* Comparison of intestinal lengthening procedures for patients with short bowel syndrome. Ann Surg **246,** 593; discussion 601, 2007.
8. Lao, O.B., Healey, P.J., Perkins, J.D., Horslen, S., Reyes, J.D., and Goldin, A.B. Outcomes in children after intestinal transplant. Pediatrics **125,** e550, 2010.
9. Park, J., Puapong, D.P., Wu, B.M., Atkinson, J.B., and Dunn, J.C. Enterogenesis by mechanical lengthening: morphology and function of the lengthened small intestine. J Pediatr Surg **39,** 1823, 2004.
10. Safford, S.D., Freemerman, A.J., Safford, K.M., Bentley, R., and Skinner, M.A. Longitudinal mechanical tension induces growth in the small bowel of juvenile rats. Gut **54,** 1085, 2005.
11. Stark, R., Panduranga, M., Carman, G., and Dunn, J.C. Development of an endoluminal intestinal lengthening capsule. J Pediatr Surg **47,** 136, 2012.
12. Spencer, A.U., Sun, X., El-Sawaf, M., Haxhija, E.Q., Brei, D., Luntz, J., *et al.* Enterogenesis in a clinically feasible model of mechanical small-bowel lengthening. Surgery **140,** 212, 2006.
13. Koga, H., Sun, X., Yang, H., Nose, K., Somara, S., Bitar, K.N., *et al.* Distraction-induced intestinal enterogenesis: preservation of intestinal function and lengthening after reimplantation into normal jejunum. Ann Surg **255,** 302, 2012.
14. Chang, P.C., Mendoza, J., Park, J., Lam, M.M., Wu, B., Atkinson, J.B., *et al.* Sustainability of mechanically lengthened bowel in rats. J Pediatr Surg **41,** 2019, 2006.
15. Okawada, M., Mustafa Maria, H., and Teitelbaum, D.H. Distraction induced enterogenesis: a unique mouse model using polyethylene glycol. J Surg Res **170,** 41, 2011.
16. Lee, G., Goretsky, T., Managlia, E., Dirisina, R., Singh, A.P., Brown, J.B., *et al.* Phosphoinositide 3-kinase signaling mediates beta-catenin activation in intestinal epithelial stem and progenitor cells in colitis. Gastroenterology **139,** 869, 2010.
17. Spencer, A., Yang, H., Haxhija, E., Wildhaber, B., Greenson, J., and Teitelbaum, D. Reduced severity of a mouse colitis model with angiotensin converting enzyme inhibition. Dig Dis Sci **52,** 1060, 2007.
18. Burgess-Cassler, A., Johansen, J.J., Santek, D.A., Ide, J.R., and Kendrick, N.C. Computerized quantitative analysis of coomassie-blue-stained serum proteins separated by two-dimensional electrophoresis. Clin Chem **35,** 2297, 1989.
19. Smith, P.K., Krohn, R.I., Hermanson, G.T., Mallia, A.K., Gartner, F.H., Provenzano, M.D., *et al.* Measurement of protein using bicinchoninic acid. Anal Biochem **150,** 76, 1985.
20. Hu, K., Ji, L., Applegate, K.T., Danuser, G., and Waterman-Storer, C.M. Differential transmission of actin motion within focal adhesions. Science **315,** 111, 2007.
21. Brady, G.F., Galban, S., Liu, X., Basrur, V., Gitlin, J.D., Elenitoba-Johnson, K.S., *et al.* Regulation of the copper chaperone CCS by XIAP-mediated ubiquitination. Mol Cell Biol **30,** 1923, 2010.
22. Feng, Y., Sun, X., Yang, H., and Teitelbaum, D.H. Dissociation of E-cadherin and β-catenin in a mouse model of total parenteral nutrition: a mechanism for the loss of epithelial cell proliferation and villus atrophy. J Physiol **587,** 641, 2009.
23. Ignatoski, K.M. Immunoprecipitation and western blotting of phosphotyrosine-containing proteins. Methods Mol Biol **124,** 39, 2001.
24. Katsumi, A., Orr, A.W., Tzima, E., and Schwartz, M.A. Integrins in mechanotransduction. J Biol Chem **279,** 12001, 2004.
25. DuFort, C.C., Paszek, M.J., and Weaver, V.M. Balancing forces: architectural control of mechanotransduction. Nat Rev Mol Cell Biol **12,** 308, 2011.
26. Craig, D.H., Haimovich, B., and Basson, M.D. Alpha-actinin-1 phosphorylation modulates pressure-induced colon cancer cell adhesion through regulation of focal adhesion kinase-Src interaction. Am J Physiol Cell Physiol **293,** 26, 2007.

27. Mitra, S.K., Hanson, D.A., and Schlaepfer, D.D. Focal adhesion kinase: in command and control of cell motility. Nat Rev Mol Cell Biol **6,** 56, 2005.
28. Ray, R.M., McCormack, S.A., Covington, C., Viar, M.J., Zheng, Y., and Johnson, L.R. The requirement for polyamines for intestinal epithelial cell migration is mediated through Rac1. J Biol Chem **278,** 13039, 2003.
29. Chauhan, B.K., Lou, M., Zheng, Y., and Lang, R.A. Balanced Rac1 and RhoA activities regulate cell shape and drive invagination morphogenesis in epithelia. Proc Natl Acad Sci U S A **108,** 18289, 2011.
30. Smith, M.A., Blankman, E., Gardel, M.L., Luettjohann, L., Waterman, C.M., and Beckerle, M.C. A zyxin-mediated mechanism for actin stress fiber maintenance and repair. Dev Cell **19,** 365, 2010.
31. Honda, K., Yamada, T., Endo, R., Ino, Y., Gotoh, M., Tsuda, H., *et al.* Actinin-4, a novel actin-bundling protein associated with cell motility and cancer invasion. J Cell Biol **140,** 1383, 1998.
32. Deschner, J., Hofman, C.R., Piesco, N.P., and Agarwal, S. Signal transduction by mechanical strain in chondrocytes. Curr Opin Clin Nutr Metab Care **6,** 289, 2003.
33. Iqbal, J., and Zaidi, M. Molecular regulation of mechanotransduction. Biochem Biophys Res Commun **328,** 751, 2005.
34. Ruwhof, C., and van der Laarse, A. Mechanical stress-induced cardiac hypertrophy: mechanisms and signal transduction pathways. Cardiovasc Res **47,** 23, 2000.
35. Geiger, B., Spatz, J.P., and Bershadsky, A.D. Environmental sensing through focal adhesions. Nat Rev Mol Cell Biol **10,** 21, 2009.
36. Zhang, S., Han, J., Sells, M.A., Chernoff, J., Knaus, U.G., Ulevitch, R.J., *et al.* Rho family GTPases regulate p38 mitogen-activated protein kinase through the downstream mediator Pak1. J Biol Chem **270,** 23934, 1995.
37. Diehl, K.M., Grewal, N., Ethier, S.P., and Woods-Ignatoski, K.M. p38MAPK-activated AKT in HER-2 overexpressing human breast cancer cells acts as an EGF-independent survival signal. J Surg Res **142,** 162, 2007.
38. Feng, Y., McDunn, J.E., and Teitelbaum, D.H. Decreased phospho-Akt signaling in a mouse model of total parenteral nutrition: a potential mechanism for the development of intestinal mucosal atrophy. Am J Physiol Gastrointest Liver Physiol **298,** G833, 2010.
39. Hoffman, B.D., Grashoff, C., and Schwartz, M.A. Dynamic molecular processes mediate cellular mechanotransduction. Nature **475,** 316, 2011.
40. Meyer, C.J., Alenghat, F.J., Rim, P., Fong, J.H., Fabry, B., and Ingber, D.E. Mechanical control of cyclic AMP signalling and gene transcription through integrins. Nat Cell Biol **2,** 666, 2000.
41. Miyasaka, E.A., Okawada, M., Utter, B., Mustafa-Maria, H., Luntz, J., Brei, D., *et al.* Application of distractive forces to the small intestine: defining safe limits. J Surg Res **163,** 169, 2010.
42. Jabaji, Z., Stark, R., and Dunn, J.C. Regeneration of enteric ganglia in mechanically lengthened jejunum after restoration into intestinal continuity. J Pediatr Surg **48,** 118, 2013.
43. Sukhotnik, I., Mogilner, J.G., Pollak, Y., Blumenfeld, S., Bejar, J., and Coran, A.G. PDGF-alpha stimulates intestinal epithelial cell turnover after massive small bowel resection in a rat. Am J Physiol Gastrointest Liver Physiol **302,** 29, 2012.
44. Chen, C.S., Tan, J., and Tien, J. Mechanotransduction at cell-matrix and cell-cell contacts. Annu Rev Biomed Eng **6,** 275, 2004.
45. Chaturvedi, L.S., Gayer, C.P., Marsh, H.M., and Basson, M.D. Repetitive deformation activates Src-independent FAK-dependent ERK motogenic signals in human Caco-2 intestinal epithelial cells. Am J Physiol Cell Physiol **294,** 9, 2008.
46. Kovalenko, P.L., Kunovska, L., Chen, J., Gallo, K.A., and Basson, M.D. Loss of MLK3 signaling impedes ulcer healing by modulating MAPK signaling in mouse intestinal mucosa. Am J Physiol Gastrointest Liver Physiol **303,** 23, 2012.
47. Livant, D.L. Targeting invasion induction as a therapeutic strategy for the treatment of cancer. Curr Cancer Drug Targets **5,** 489, 2005.
48. Kallergi, G., Agelaki, S., Markomanolaki, H., Georgoulias, V., and Stournaras, C. Activation of FAK/PI3K/Rac1 signaling controls actin reorganization and inhibits cell motility in human cancer cells. Cell Physiol Biochem **20,** 977, 2007.
49. Liu, W.F., Nelson, C.M., Tan, J.L., and Chen, C.S. Cadherins, RhoA, and Rac1 are differentially required for stretch-mediated proliferation in endothelial versus smooth muscle cells. Circ Res **101,** e44, 2007.
50. Swanson, P.A., 2nd., Kumar, A., Samarin, S., Vijay-Kumar, M., Kundu, K., Murthy, N., *et al.* Enteric commensal bacteria potentiate epithelial restitution via reactive oxygen species-mediated inactivation of focal adhesion kinase phosphatases. Proc Natl Acad Sci U S A **108,** 8803, 2011.
51. Bouchard, V., Demers, M.J., Thibodeau, S., Laquerre, V., Fujita, N., Tsuruo, T., *et al.* Fak/Src signaling in human intestinal epithelial cell survival and anoikis: differentiation state-specific uncoupling with the PI3-K/Akt-1 and MEK/Erk pathways. J Cell Physiol **212,** 717, 2007.
52. Zhong, X., and Rescorla, F.J. Cell surface adhesion molecules and adhesion-initiated signaling: understanding of anoikis resistance mechanisms and therapeutic opportunities. Cell Signal **24,** 393, 2012.
53. Flanigan, T.L., Owen, C.R., Gayer, C., and Basson, M.D. Supraphysiologic extracellular pressure inhibits intestinal epithelial wound healing independently of luminal nutrient flow. Am J Surg **196,** 683, 2008.
54. Gayer, C.P., and Basson, M.D. The effects of mechanical forces on intestinal physiology and pathology. Cell Signal **21,** 1237, 2009.
55. Ralls, M.W., Sueyoshi, R., Herman, R., Utter, B., Czarnocki, I., Luntz, J., *et al.* Development of a novel approach to safely couple the intestine to a distraction-induced device for intestinal growth: use of reconstructive tissue matrix. Pediatr Surg Int **29,** 151, 2013.
56. Shekherdimian, S., Scott, A., Chan, A., and Dunn, J.C. Intestinal lengthening in rats after massive small intestinal resection. Surgery **146,** 291, 2009.

Address correspondence to:
*Daniel Teitelbaum, MD*
*Section of Pediatric Surgery*
*Department of Surgery*
*Mott Children's Hospital*
*University of Michigan*
*1540 E. Hospital Dr., SPC 4211*
*Ann Arbor, MI 48109-4211*

*E-mail:* dttlbm@umich.edu

*Received: June 27, 2013*
*Accepted: September 25, 2013*
*Online Publication Date: November 5, 2013*

**This article has been cited by:**


1. Joshua D. Rouch, James C. Y. Dunn. 2017. New Insights and Interventions for Short Bowel Syndrome. *Current Pediatrics Reports* **5**:1, 1-5. [Crossref]
2. Kurodo Koshino. 2015. Novel isolated cecal pouch model for endoscopic observation in rats. *World Journal of Gastroenterology* **21**:17, 5242. [Crossref]